Fission Neutron Spectrum of U^{235}†

L. CRANBERG, G. FRYE, N. NERESON, AND L. ROSEN
University of California, Los Alamos Scientific Laboratory, Los Alamos, New Mexico
(Received April 30, 1956)

The neutron spectrum associated with the fission of U^{235} induced by slow neutrons has been remeasured from 0.18 to 12 Mev. Two different experimental techniques were employed in this measurement: (1) the time-of-flight method covering the energy range from 0.18 to 2.7 Mev, and (2) the photographic plate method encompassing the energy range from 0.35 to 12 Mev. The combined results of these measurements fit the relation, $N(E)=Ke^{-E/0.965}\sinh[(2.29E)^{\frac{1}{2}}]$, where $N(E)$ is the neutron flux, E is the neutron energy in Mev and K is a constant. The simpler expression, $N(E)=KE^{\frac{1}{2}}e^{-0.775E}$, also fits the data well for neutron energies below 9 Mev.

I. INTRODUCTION

SEVERAL studies on the neutron spectrum resulting from thermal fission of U^{235} were carried out in 1948 and 1949 and were reported in the literature in 1951 and 1952.[1–4] A remeasurement of the fission spectrum at the present time seemed desirable for several reasons: (1) all of the above measurements assumed that room background was negligible compared to other experimental errors, whereas the present experiment shows that this assumption is justified only for energies $>\sim 2$ Mev; (2) more reliable spectral data can be obtained at the present time owing to the improvement in nuclear spectroscopy techniques; also, more precise data on the neutron cross section of hydrogen are now available for use with the nuclear plate method; (3) since the fission spectrum is the starting point for all calculations on nuclear reactors, an accurate knowledge of this function has become more important with the increasing application of nuclear reactors.

This remeasurement of the spectrum especially emphasized (1) a simple experimental arrangement with the U^{235} source and the neutron detector clear of large scattering objects, (2) an accurate determination of room scattered background, and (3) the determination of the spectrum over a large energy range for comprehensively checking the fit of empirical formulas with the experimental data. The reliability of the data over the energy region where most of the fission neutrons occur (0.5 to 3 Mev) was further strengthened by employing two quite different measurement techniques.

II. EXPERIMENTAL

In order to cover as large an energy range as possible, both the photographic plate method and the time-of-flight method were utilized in remeasuring the U^{235} fission neutron spectrum. The nuclear plate method contributing the major portion of the information by providing data over the energy region from 0.35 to 12 Mev. The time-of-flight technique covered the energy region from 0.18 to 2.7 Mev. It served to extend the spectrum down to a lower energy and provided an independent check on the nuclear plate data over the most important region of the spectrum. These two methods are conveniently normalized to each other as they both provide data over a common energy interval of about 2.5 Mev. The experimental procedure and results from each of the above two methods are discussed separately in the following sections.

A. Photographic Plate Method

In this method, Ilford C-2 emulsions of 200 μ thickness were used to detect the neutrons and measure their energies. This technique is adequately discussed in a review article[5] by one of the authors. The chief differences in this experimental method as compared to that usually applied are as follows:

(1) To increase the accuracy with which dip angle could be measured, the plates were soaked in a 15% glycerine solution to minimize shrinkage.

(2) The orientation of each proton recoil trajectory with respect to the incident neutron direction was determined. This permitted a determination of the energy of each neutron from the energy of the corresponding proton recoil. (The usual procedure is to accept proton recoils within a given angular criteria, measure the projection in the plane of the emulsion of the ranges of the recoil protons, and make an average correction to the deduced neutron energies.)

(3) Although only 10 000 tracks were analyzed, the statistical accuracy at the high-energy end of the spectrum was considerably improved by scanning a large volume of emulsion for tracks which represent neutrons of energy greater than 4 Mev, while ignoring the lower energy proton recoils. This procedure was useful because of the variation with energy of the fission spectrum, the n-p scattering cross section, and the probability of tracks remaining within the emulsions. All these factors serve to reduce markedly the number of acceptable high-energy proton recoil tracks.

† This work was performed under the auspices of the U. S. Atomic Energy Commission.
[1] Bonner, Ferrell, and Rinehart, Phys. Rev. **87**, 1032 (1952).
[2] David L. Hill, Phys. Rev. **87**, 1034 (1952).
[3] B. E. Watt, Phys. Rev. **87**, 1037 (1952).
[4] Norris Nereson, Phys. Rev. **85**, 600 (1952).
[5] L. Rosen, Nucleonics **11** (No. 7), 32 (1953).

For example, in the case of the fission spectrum, the ratio of acceptable proton recoils at 1 Mev to the corresponding number at 10 Mev is approximately 3000:1.

(4) The plate analyses were confined to a region 2 to 4 mm from the edge of the plate nearest the neutron source. This was done to avoid excessive selective attenuation[5] of the neutron beam by the emulsion and glass backing.

The experimental arrangement for measuring the thermal fission spectrum of U^{235} is schematically illustrated in Fig. 1. The Los Alamos water boiler reactor was used as the source of thermal neutrons. By using a vertical reactor port instead of a side port, the room background was reduced, since only one heavy shielding face instead of two was present which would allow neutrons from the U^{235} fission foil to be reflected back into the detector. Care was taken to isolate the detector and fissionable material from scattering objects by using a light support for the fission foil and by making the distance large from the top reactor shield to the experimental units. The geometry was such as to provide an angular resolution of $\pm 5°$ between source and detector. A series of six runs were made; three of these were data runs and three were background runs in which a truncated pyramid of polyethylene was interposed between the U^{235} foil and the detector.

The plates were surrounded by cadmium to inhibit thermal-neutron-induced $N^{14}(n,p)C^{14}$ reactions in the emulsion, since protons from this reaction have an energy of approximately 0.6 Mev and are indistinguishable from proton recoils of the same energy. Thermal neutrons in the vicinity of the detectors are due to the following causes: (1) scattering of the thermal neutron beam in the U^{235} plate (the background run cannot, of course, be used to correct for this source of background); (2) fission neutrons degraded in energy by room scattering. Aside from thermal neutron background, one is obliged to contend with a significant number of neutrons whose energy is in the region in which data are to be taken, which do not come directly from the fission plate to the detector. Such neutrons distort the observed fission spectrum for they appear as degraded neutrons. The preponderance of low-energy neutrons (<1 Mev) in the background spectrum as compared to the fission spectrum, is due to (1) the fact that a good many of the room-scattered neutrons have indeed been degraded by the scattering (especially inelastic) process, and (2) the fact that these neutrons impinge on the plate at large angles with respect to the assumed direction of incidence of neutrons on the detector. The room-scattered background can be taken into account by the procedure mentioned above of making runs with and without a shadow scatterer between source and detector. The background spectrum thus obtained is multiplied by the factor $(1+\Omega/4\pi)$,

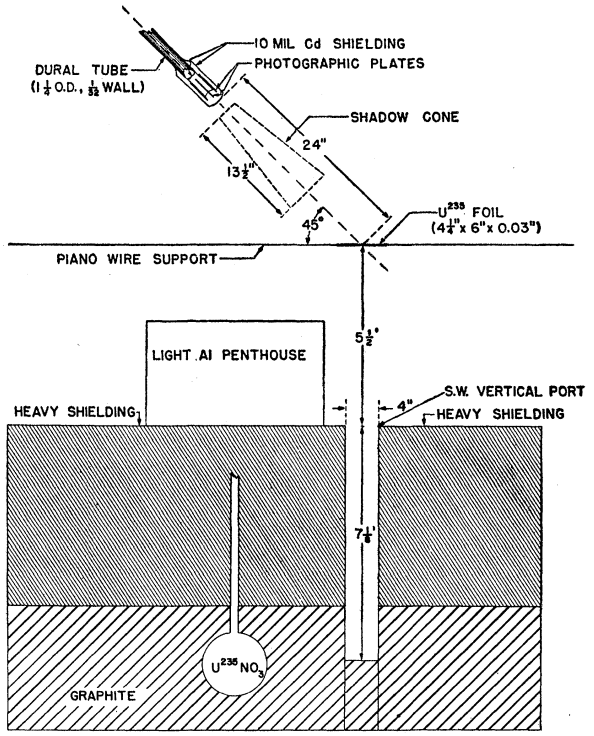

FIG. 1. Experimental arrangement for photographic plate method.

where Ω is the solid angle subtended by the pyramid at the detector, and then is subtracted from the "run" spectrum. This background correction amounted to 14% at 0.3 Mev, 6% at 0.5 Mev, 3% at 1.0 Mev, and 1% at 2.0 Mev.

It has been shown[5] that high-energy neutrons produce (n, charged particle) reactions in the emulsion, the tracks of which are for the most part indistinguishable from proton recoils; at 14 Mev this effect is approximately 10%. However, since the fission spectrum exhibits relatively few high-energy neutrons, the interaction of a small fraction of these in the emulsion to produce charged particles which have the appearance of proton recoils due to low-energy neutrons will have a completely negligible effect on the neutron spectrum.

Finally, there existed the possibility that the thermal neutron beam might be contaminated by neutrons of higher energy which could be scattered into the detector by the U^{235} plate. Such neutrons would not be included in the above background correction. In order to clear up this point, cadmium ratio measurements were made on the "thermal" beam. This ratio proved to be 106:1. This means that if we take into account the transmission of the U^{235} plate for 0.3-Mev neutrons (the lowest energy at which data were taken in this experiment), one arrives at a contribution to the fission spectrum from this effect of less than 0.1%.

The nuclear plate data and its treatment to obtain the fission neutron spectrum of U^{235}, $N(E)$, are shown in Table I. The errors in $N(E)$ shown in the right-hand

TABLE I. Data and results from photographic plate method.[a]

E (Mev)	E_i (Mev)	N_p	VW (mm³)	σ_{n-p} (barns)	$\bar{p}$	$N(E)_{\text{run}}$	$N(E)_{bg}$	$N(E)$	$N(E)/\sqrt{E}$	S.E. (%)
0.35	0.3– 0.4	452	12.75	7.65	1.00	960.6	137.8	823	1391	4.7
0.5	0.4– 0.6	1228	21.46	6.30	1.00	901.0	51.3	850	1204	3.1
0.7	0.6– 0.8	1156	23.31	5.28	1.01	900.5	30.1	870	1040	3.1
0.9	0.8– 1.0	863	23.43	4.57	1.01	780.0	26.4	754	795	3.7
1.1	1.0– 1.2	777	23.43	4.05	1.01	794.0	19.3	775	738	3.7
1.3	1.2– 1.4	683	23.43	3.72	1.02	775.6	10.3	765	671	3.9
1.5	1.4– 1.6	543	23.43	3.42	1.02	673.9	11.1	663	541	4.4
1.7	1.6– 1.8	453	23.43	3.20	1.03	601.6	9.0	593	455	4.8
1.9	1.8– 2.0	378	23.43	3.00	1.03	536.4	1.6	535	388	5.2
2.1	2.0– 2.2	329	23.43	2.85	1.04	497.2	6.6	491	339	6.2
2.3	2.2– 2.4	304	24.65	2.75	1.04	456.5	6.9	450	297	6.6
2.5	2.4– 2.6	276	24.65	2.60	1.05	437.9	3.8	434	275	6.1
2.7	2.6– 2.8	210	24.65	2.50	1.05	350.0	0.0	350	213	6.9
2.9	2.8– 3.0	170	24.65	2.40	1.06	295.4	0.0	296	174	7.7
3.1	3.0– 3.2	146	24.65	2.25	1.07	273.5	2.3	271	154	8.5
3.3	3.2– 3.4	139	24.65	2.16	1.08	271.5	2.3	269	148	8.6
3.5	3.4– 3.6	125	24.65	2.07	1.08	258.8	2.4	256	137	9.1
3.7	3.6– 3.8	93	24.65	2.00	1.09	202.1	2.6	200	104	10.6
3.9	3.8– 4.0	152	43.85	1.93	1.10	219.5	0.0	219	111	8.1
4.2	4.0– 4.4	255	53.10	1.83	1.12	143.5	4.3	139	67.8	6.2
4.6	4.4– 4.8	320	92.65	1.72	1.14	116.7	0.0	117	54.6	5.6
5.0	4.8– 5.2	269	113.22	1.62	1.16	85.9	0.0	85.9	38.4	6.1
5.4	5.2– 5.6	269	159.17	1.53	1.19	67.6	1.7	65.9	28.4	6.1
5.8	5.6– 6.0	244	211.11	1.46	1.21	49.3	0.0	49.3	20.5	6.4
6.2	6.0– 6.4	185	211.11	1.38	1.25	40.3	0.0	40.3	16.2	7.4
6.6	6.4– 6.8	121	211.11	1.32	1.28	28.7	0.0	28.7	11.2	9.1
7.0	6.8– 7.2	79	211.11	1.26	1.32	20.2	0.0	20.2	7.65	11.2
7.4	7.2– 7.6	54	211.11	1.20	1.37	15.1	0.0	15.1	5.55	13.5
7.8	7.6– 8.0	51	211.11	1.16	1.42	12.6	0.0	12.6	4.52	15.6
8.4	8.0– 8.8	49	211.11	1.09	1.53	6.8	0.0	6.8	2.34	14.3
9.2	8.8– 9.6	10	211.11	1.00	1.68	2.0	0.0	2.0	0.66	31.2
10.0	9.6–10.4	9	211.11	0.930	2.06	2.1	0.0	2.1	0.66	33.3
10.8	10.4–11.2	4	211.11	0.865	2.38	1.4	0.0	1.4	0.43	50
12.0	11.2–12.8	2	211.11	0.792	2.88	0.48	0.0	0.48	0.14	70

[a] The symbols have the following meaning: E—mean neutron energy; E_i—neutron energy interval corresponding to E; N_p—number of proton recoils measured in the proton energy interval corresponding to E_i; VW—the product of emulsion volume and neutron flux incident on detectors; σ_{n-p}—the n-p scattering cross section; $\bar{p}$—the correction for knock-on protons leaving the emulsion surfaces; $N(E)_{\text{run}}$—the number of neutrons per cm² per Mev $\times 2 \times 10^{-5}$ at energy E including background neutrons; $N(E)_{bg}$—the neutron energy distribution with polyethylene pyramid interposed between source and detector; $N(E) = [N(E)_{\text{run}} - N(E)_{bg}]$—neutron energy distribution from thermal neutron fission of U^{235}; S.E.—statistical error in $N(E)$ expressed in percent of $N(E)$.

column are calculated from statistics alone. Relative errors arise from three sources: (1) determination of the solid angle of acceptance of proton recoils, (2) hydrogen content of the emulsion volume analyzed, (3) n-p scattering cross section. These combine to give the following total relative errors over the various energy regions of the spectrum, 0.3–0.4 Mev, 15%, 0.4–0.9 Mev, 6%, 0.9–3.0 Mev, 4%, above 3 Mev, 5%. These values reflect the fact that (1) and (2) are random uncertainties and that fourteen analysts worked on the eleven plates used for this spectrum. The above spectral data are further discussed with similar results from the time-of-flight method in the last section.

B. Time-of-Flight Method[6]

1. Experimental Arrangement

A diagram of the apparatus for the time-of-flight method for measuring the fission neutron spectrum of U^{235} is shown in Fig. 2. The experiment was carried out with the large Los Alamos Van de Graaff accelerator as the source of neutrons for bombarding the U^{235}. A spiral fission chamber[7] containing U^{235} served as the source of fission neutrons. The detector for the fission neutrons emerging from this chamber consisted of "Scintilon" plastic mounted on a photomultiplier tube. The energies of the neutrons were determined by measuring their time of flight from the fission chamber to the scintillator.

The neutrons were generated by the $Li^7(p,n)Be^7$ reaction. They were in the energy range 5 to 80 kev, corresponding to a proton energy of 1.90 Mev, a lithium target thickness of 15 kev, and a range of angle subtended by the fission chamber at the target of $\pm 25°$. By tickling the threshold of an endothermic reaction, low-energy neutrons are produced in a forward cone, thus making it possible to keep the fission-neutron detector out of the direct neutron flux

[6] For further details concerning this experiment see L. Cranberg and N. Nereson, Los Alamos Report LA-1916 (unpublished).

[7] B. Rossi and H. Staub, *Ionization Chambers and Counters* (McGraw-Hill Book Company, Inc., New York, 1949).

from the target without use of shield or collimator. Choice of the $Li^7(p,n)Be^7$ reaction was based on yield and ease of operating the accelerator at the threshold energy of the reaction. The choice of target conditions represented a rough compromise between yield and detector background counts. The detector background came mainly from counts in the scintillator which were due to target neutrons elastically scattered by the fission chamber. Under the conditions chosen, these neutrons were all on the low-energy tail of the detector sensitivity curve.

The spiral fission chamber was selected as the fission neutron source in order to provide a zero-time pulse for the neutron time-of-flight measurement. The chamber used had a rise time (10 to 90%) of about 2×10^{-8} sec, which was adequate for the timing requirements of the present experiment. The chamber contained about 1 g of U^{235} in the form of UO_3 coated on approximately 10 spiral turns of platinum foil 1 mil thick. The gas filling was commercial argon at a pressure of 80 psi. The wall of the chamber was brass 20 mils thick, and its outside dimensions were: diameter, $\frac{7}{8}$ inch, depth 1 inch. The center of the fission chamber was placed about 1 inch from the lithium target.

One must take account of the possibility that, with the thick layers of fissionable material used in these experiments, those fission events might be favored whose fragments were oriented perpendicularly to the layers. If these layers were not oriented randomly in relation to the detector, the data might represent a weighting for or against certain directions of fragment emission. Since the velocities of the fragments strongly influence the spectrum of neutrons emitted by them, particularly at low energies, the observed spectrum might be distorted from that for random orientation. To randomize the layer orientation relative to the detector axis as much as possible, the axis of the spiral was perpendicular to the direction of neutron detection. Further assurance against intrusion of disturbing effects from this source is obtained if the efficiency for detection of fission events in the chamber is high. The chamber was operated at such a bias that noise counts were a few per second. At this bias subsequent experiments gave a detection efficiency for this chamber of about 40%.

The photomultiplier pulse furnished the second timing signal for measurement of the flight-of-time of the fission neutrons. "Scintilon" plastic, which detects neutrons by proton recoil, possessed several desirable features for this experiment: (1) it has a large hydrogen content, (2) gives good light signals for low-energy neutrons, and (3) is conveniently available in large sizes. The plastic ($1\frac{3}{4}$ in. in diam and 1 in. thick) was mounted on an RCA 6342 photomultiplier tube. A mu-metal shield was placed around the tube to minimize effects produced by earth's magnetic field and the field of the accelerator analyzing magnet.

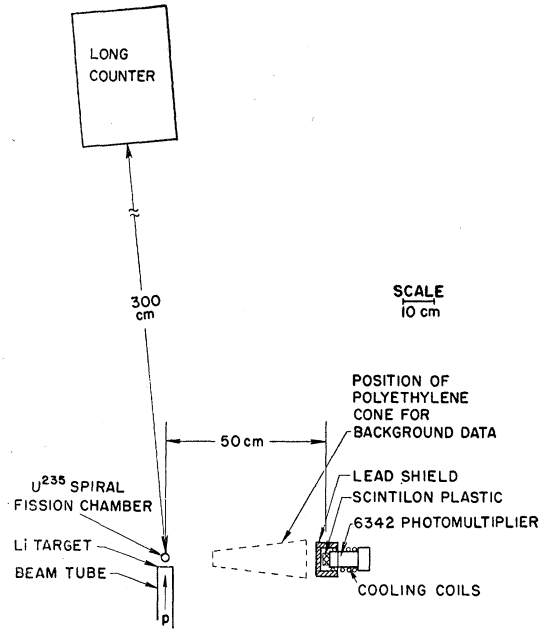

FIG. 2. Experimental arrangement for time-of-flight method.

In order to reduce the sensitivity of the detector to cosmic-ray background, room-scattered neutrons and gamma rays and fission gamma rays, a cylindrical lead shield with one end closed was placed over the crystal; the wall thickness of the cylinder and the end thickness were each $\frac{1}{2}$ inch.

In order to improve the signal-to-noise ratio for low-energy neutrons, the photomultiplier tube was cooled to a temperature of 0°C. This reduced the noise background by a factor of 3 compared to that obtained at room temperature for the operating bias used in the experiment. This noise background was about 3000 counts/min, which was about $\frac{1}{10}$ the scintillator rate prevailing during the spectrum measurements.

Precautions were taken to eliminate large masses of material from the immediate vicinity of the experimental components which could scatter fission neutrons into the detector and thereby degrade the fission spectrum. The object closest to the spiral chamber consisted essentially of the tantalum target disk, 0.010 in. thick. The nearest large object was the $\frac{3}{16}$ in. thick steel floor which was located 5 feet below the target and detector. However, as in the photographic plate method, air scattering and room-scattered background from distant objects were still possibilities. Therefore, as in the previous method, background runs were taken with a polyethylene cone one foot long inserted between the source and detector.

A long counter was used to monitor the neutrons from the Van de Graaff target. This counter was located slightly off the beam-tube axis and about 3 meters from the target.

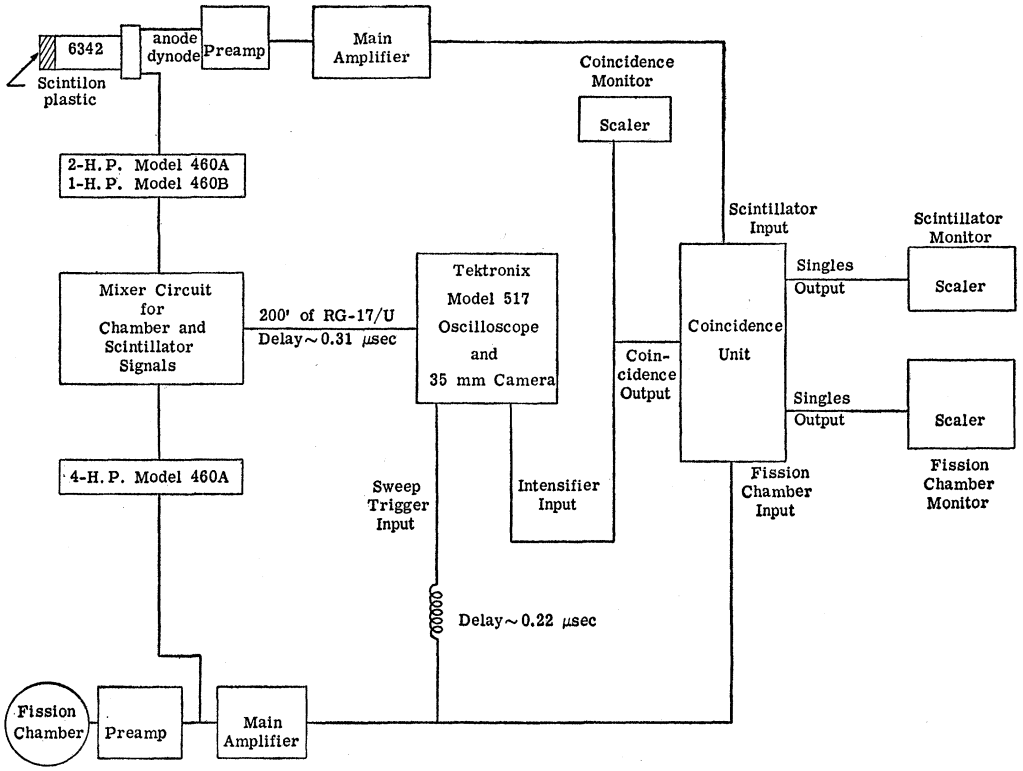

FIG. 3. Instrumentation diagram for time-of-flight experiment.

2. Electronic Instrumentation

The time, t, for a neutron of velocity v to travel s cm is given by $t=s/1.39E^{\frac{1}{2}}\times10^{9}$, where E is in Mev. Since s was 50 cm in this experiment, $t^2=12.92/E$, where t is in units of 10^{-8} sec and E in Mev. For the neutron energy range measured in this experiment, 0.16 to 3.2 Mev, the corresponding time-interval range is 9×10^{-8} to 2×10^{-8} sec.

A block diagram of the electronic components employed in the experiment is shown in Fig. 3. A fast amplifier system is used for those signals on which time measurements are made; a parallel slow system selects the events to be observed. The fast pulse system amplified the chamber and scintillator signals with Hewlett-Packard Model 460A amplifiers and combined them in a mixer circuit. The common output of the mixer circuit was fed through about 200 ft of RG-17/U cable (for delay purposes) into the signal input of a Tektronix Model 517 oscilloscope. The combined signals were displayed on the 0.02-μsec/cm sweep of the oscilloscope and photographed on 35 mm Linagraph Pan film. To aid in distinguishing the two signals from each other, the sign of the scintillator pulse was inverted by introducing a Hewlett-Packard 460B unit into its amplifier system.

The "slow" pulse system used slower amplifiers (10 to 90% rise time ~0.06 μsec) to bring the chamber and photomultiplier signals together in a coincidence unit having a resolving time of 0.15 μsec. The output coincidence signal was used to trigger the intensifier of the oscilloscope. Thus, no time measurement was made unless the chamber and photomultiplier pulses occurred within 0.15 μsec of each other. In order to be certain that small signals originating from low-energy fission neutrons would not be missed the coincidence time interval was made considerably longer than that dictated by the maximum flight time intervals of 9×10^{-8} sec. The RG-17/U cable in the fast mixed-signal line was used to compensate for the difference between the transit times in the fast and slow systems.

Each time a fission event occurred the sweep of the 517 oscilloscope was started by the discriminator signal from the fission chamber side of the coincidence unit. The sweep would not be visible, of course, unless the intensifier or coincidence signal was also present. Since the display signal to the 517 was delayed, it was also necessary to insert a delay in the sweep trigger pulse in addition to that inherently present in the fission chamber slow amplifier, coincidence unit, and the oscilloscope circuits. An additional delay in the form of a long cable was inserted in the photomultiplier dynode signal; this delay increased the separation of the scintillator and chamber pulses and simplified reading of the data.

The film traces of the final data showed that the uncertainty in determining the start of the fission

chamber signal was approximately $\pm 0.4\times10^{-8}$ sec. This uncertainty was largely determined by the signal to noise ratio of the chamber pulse. Because the "noise" decreased by about a factor of 2 when the polarizing voltage was removed from the chamber, the predominant "noise" was interpreted as due to alphas from the decay of U^{235}. The beginning of the scintillator pulse could be established within $\pm 0.1\times10^{-8}$ sec due to its faster rise time. Because of the spread in photomultiplier transit times, the arrival of the photomultiplier output signal may sometimes lag the neutron arrival by 0.2 or 0.3×10^{-8} sec.[8] Therefore, a total uncertainty of about $\pm 0.5\times10^{-8}$ sec may be expected in the measurement of the flight time of the fission neutrons. This provides adequate energy resolution ($\sim$15%) over the low-energy region of the spectrum where the contribution from this method is most valuable.

3. Detector Energy Sensitivity

To determine the relative efficiency of the "Scintilon" plastic as a function of neutron energy, its response to monochromatic neutrons of various known energies was compared to that of a long counter, and it was assumed that the long-counter response is flat with energy in the region of interest.[9]

The calibration arrangement is shown at the top of Fig. 4. The long counter and scintillator were set up a few degrees to each side of the axis of the beam-tube, and placed at such a distance that each detector subtended approximately the same solid angle at the target. This procedure insured that each detector was exposed to neutrons of the same number and energy at the various energies. The discriminator output on the scintillator side of the coincidence unit was used to obtain the scintillator counts in the calibration measurements, the same bias being used as in the running of the spectral data.

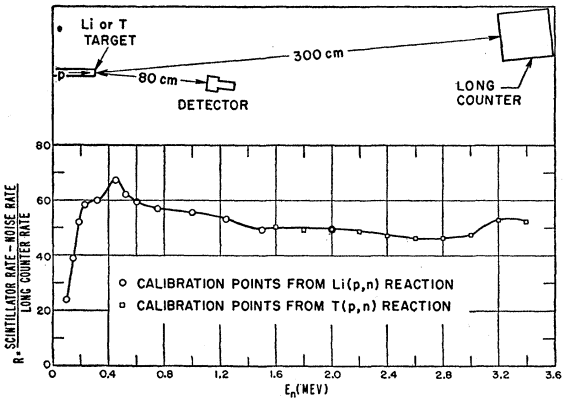

FIG. 4. Arrangement for calibrating scintillator detector and results.

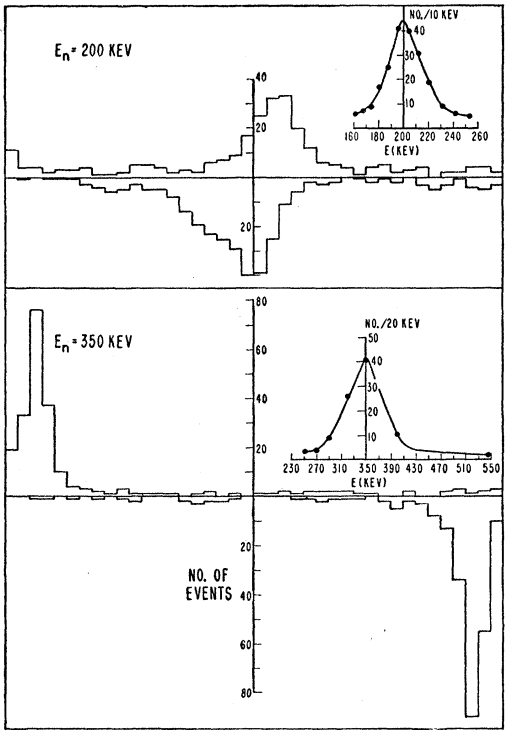

FIG. 5. Response of scintilon plastic to low-energy monochromatic neutrons.

The (p,n) reaction in Li was used to calibrate the scintillator over the neutron energy range 0.1 to 2.0 Mev both before and after a run on the spectral data. A small correction is necessary for the second group of neutrons which appears in the lithium reaction above a proton energy of 2.38 Mev. The (p,n) reaction in tritium was later used to extend the calibration to 3.4 Mev. During these calibrations the target thickness for protons was held under 3 kev.

With the proton beam deflected from the target, the counting rates in the scintillator and long counter amounted to less than 2% of the calibration counting rate. The calibration measurements were further checked for background by placing a polyethylene cone 1 foot long in front of the target. Since backgrounds were about 5% for both scintillator and long counter, corrections were negligible.

The calibration results are shown at the bottom of Fig. 4, where the ratio of scintillator to long-counter counting rate is plotted. On the assumption that the long counter is flat, this curve is the energy sensitivity curve of the scintillator. Calibration of the long counter with a polonium-beryllium neutron source gave a value of 50%, approximately, for the neutron detection efficiency of the scintillator over the flat region.

[8] These large time fluctuations occur predominantly in the case of small pulses or low-energy neutrons. For these neutrons the time-of-flight is longest and the percent error due to the average time lag is small.

[9] Previous experiments have shown that the particular long counter used in these measurements has a sensitivity which is flat to within 5% over the energy range used [R. Nobles (private communication)].

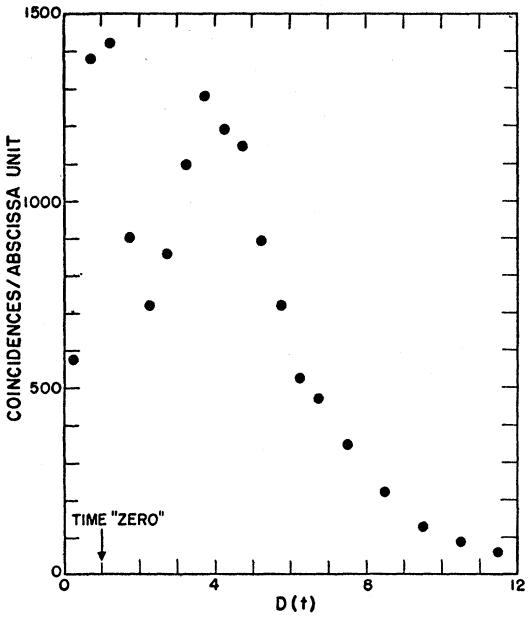

FIG. 6. Film data from time-of-flight experiment. Number of scintillator-chamber coincidences are plotted as a function of the difference, $D(t)$, between the times of scintillator and fission signals. One abscissa unit$\cong 0.8\times10^{-8}$ sec.

Experimental information concerning the energy resolution of the flight-time measurements was obtained by pulsing the proton beam of the Van de Graaff accelerator.[10] Protons striking the lithium target in bursts of duration 0.2×10^{-8} sec produced neutron bursts of the same duration. A time scale synchronized with the neutron bursts was obtained by coupling to the horizontal plates of an oscilloscope a portion of the sinusoidal signal used to pulse the proton beam; the fast scintillator pulse was displayed on the vertical plates. For these data, the fission chamber was removed and the scintillator was placed in front of the target at a distance of about 50 cm, while the Van de Graaff accelerator was pulsed to produce monochromatic neutrons of various energies. No detectable gamma-ray line appeared on the oscilloscope display along with the neutron peak. This proved that the neutron sensitivity calibration of the scintillator was not in error by more than 5% because of the presence of gamma rays.

Typical results showing the scintillator response to low energy neutrons are shown in Fig. 5. During these exposures the scintillator rate with neutrons was 9000 counts/min, the scintillator rate without neutrons (noise) was 1800 counts/min. The oscillator frequency pulsing the output of the Van de Graaff accelerator was 4.19 Mc/sec. The data are shown in two forms: first, the results obtained when the vertical projections of the beginning of the pulses on the sine wave sweep are plotted; and second, the conversion of the data of the upper trace into a plot *versus* energy. The energy graphs show that under the above conditions the resolution at 200 kev is about 15% and at 350 kev the resolution is 19%. The high noise level existing during the above exposures increased the width of these energy distributions by about 20%, and gave poorer results for the resolution than are attainable with a better signal to noise ratio.

[10] For further information concerning this technique see L. Cranberg, Los Alamos Report LA-1654 (unpublished).

4. Data

The time-of-flight data were obtained by measuring the oscilloscope sweep time interval between the leading edges of the fission chamber and photomultiplier pulses. The data taken from the film records are illustrated in Fig. 6 where the number of coincidences observed is plotted as a function of the difference between the times of scintillator and fission signals. Events under the left peak are due to gamma rays whereas fission neutrons are responsible for the broader peak to the right. Approximately 16 000 total events were recorded and, out of this total, about 10 000 were due to fission neutrons.

The center of the gamma-ray peak occurs at 1 abscissa unit which represents the "zero" of the time base, since the gamma-ray flight time was negligible compared to the time resolution of the data. The width of the gamma peak at half-maximum is about 1.4 units or slightly over 1×10^{-8} sec in time. This is in agreement with the uncertainty of $\pm0.5\times10^{-8}$ sec for the flight time estimated previously from instrumentation considerations.

The background data obtained with the polyethylene cone between the chamber and scintillator were accumulated in the same manner as the regular data. As in the photographic plate method, the background is a function of the neutron energy and in this experiment the percentage of background in the data varied from a minimum of $\sim$2% at the highest energy to a maximum of 18% at the lowest energy. (See Table II.) The calculated random coincidence rate was about $\frac{1}{3}$ of the total background. This indicated that scattering processes were responsible for the majority of the background coincidences. If one considers the entire flight-time interval of 9×10^{-8} sec, the average random coincidence rate was only about 3% of the total data coincidence rate.

Calculation of the U^{235} fission neutron spectrum from the data of Fig. 6 is shown in Table II. The data from 1.6 to 2×10^{-8} sec were not used since calibration neutrons were not available for this energy region. The error in the energy correction factors for the detector, as derived from Fig. 4, is estimated to be about 2%; this is exclusive of the error associated with the energy response of the long counter. The errors given for $N(E)$ are purely statistical. Below 1 Mev, the statistical errors combined with other instrumental errors give each point an over-all accuracy of $\pm10\%$

TABLE II. Data and results from time-of-flight method.[a]

t_i (10^{-8} sec)	E (Mev)	E_i (Mev)	$N(t)_{\text{run}}$	$N(t)_{bg}$	$B_g(\%)$	$N(t)$	$S(E)$	$N(E)$	S.E.	$N(E)/\sqrt{E}$
1.6–2.0	4.14	1.82	1099	23	2.1	1076				
2.0–2.4	2.73	0.990	1279	20	1.6	1259	1.37	1740	±50	1054
2.4–2.8	1.94	0.590	1193	20	1.7	1173	1.27	2520	±75	1811
2.8–3.2	1.46	0.390	1146	20	1.8	1126	1.21	3480	±100	2880
3.2–3.6	1.13	0.260	895	20	2.2	875	1.14	3830	±130	3610
3.6–4.0	0.905	0.190	722	20	2.8	702	1.12	4130	±160	4340
4.0–4.4	0.738	0.144	525	20	3.8	505	1.11	3890	±170	4530
4.4–4.8	0.613	0.106	471	20	4.2	451	0.95[b]	4040	±210	5150
4.8–5.7	0.480	0.158	694	40	5.8	654	1.00	4140	±160	5980
5.7–6.5	0.354	0.096	448	39	8.7	409	1.02	4350	±220	7310
6.5–7.3	0.275	0.063	255	34	13	221	1.05	3680	±250	7020
7.3–8.2	0.218	0.050	182	28	15	154	1.11	3420	±280	7340
8.2–9.1	0.175	0.037	126	23	18	103	1.21	3370	±340	8050

[a] The symbols have the following meaning: t_i—flight-time interval of U^{235} fission neutrons in units of 10^{-8} sec; E—mean neutron energy of flight-time interval; E_i—neutron energy interval corresponding to t_i; $N(t)_{\text{run}}$—number of chamber-scintillator coincidences measured in listed flight-time interval; $N(t)_{bg}$—number of chamber-scintillator coincidences measured with 1 ft polyethylene cone between chamber and scintillator; $B_g(\%)=[N(t)_{bg}/N(t)_{\text{run}}]\times 100$, or percent background; $N(t)=N(t)_{\text{run}}-N(t)_{bg}$; $S(E)$—relative inverse energy sensitivity of scintillator as derived from Fig. 4; normalized to unity at $E=0.480$ Mev; $N(E)=N(t)S(E)/E_i$—neutron energy distribution from thermal neutron fission of U^{235}; S.E.—statistical error in $N(E)$.

[b] On the basis of the scintillator energy sensitivity curve in Fig. 4, $S(E)$ at this energy should be 1.05; however, a 10% correction for the second group of target neutrons is required at this energy value.

or better. Above 1 Mev, the over-all accuracy of each point is approximately ±5%.

In converting from the measured time distribution (Fig. 6) to an energy distribution, account must be taken of the resolution function of the apparatus. The resolution function may be estimated from the uncertainty in the timing of the fission events, which is essentially the width of the fission gamma-ray line, and the results of the observations on monoenergetic neutrons with a pulsed beam. For neutrons above 0.5 Mev, the resolution width for pulsed neutrons is negligible compared to the width of the fission gamma-ray line. Below this energy, the spread in neutron detection time is approximately $\frac{1}{2}\times 10^{-8}$ sec. To equalize the effect of the resolution function over the time range, the time interval chosen for the presentation of the data were doubled for times corresponding to an energy less than 0.5 Mev. Thus, in general, the intervals chosen are of the order of $\frac{1}{2}$ or more of the resolution width. The greatest effect of the curvature of the observed time distribution on the calculated energy distribution due to the width of the resolution function is estimated to be not greater than 4%.

III. RESULTS AND DISCUSSION

The fission spectrum measurements from both experimental methods are graphically displayed in Figs. 7, 8, and 9. The time-of-flight results from Table II were multiplied by a factor[11] of 0.204 to normalize them to the photographic plate results of Table I. Figure 7 illustrates a semilogarithmic plot of the data, and it can be seen that the data are fitted over their entire range by an equation of the form $N(E)=Ke^{-E/0.965}\sinh[(2.29E)^{\frac{1}{2}}]$, where K is a constant and E, the neutron energy, is in Mev. The equation deduced by Watt[3] to fit the data of Bonner *et al.*,[1] Hill,[2] and Watt[3] had the form $e^{-E}\sinh(2E)^{\frac{1}{2}}$.

The fission spectrum can be represented by a straight line over the greater part of the energy range by plotting $\ln[N(E)/\sqrt{E}]$ *vs* E. In Fig. 8, the combined data have been plotted in the above manner. A straight line having a slope of 0.775 fits the data points best,[12] and leads to the expression, $N(E)=kE^{\frac{1}{2}}e^{-0.775E}$, for the fission spectrum. The data points above 9 Mev lie somewhat below the straight line and therefore this simpler expression should be restricted in use to fission neutron energies below 9 Mev.

A linear plot of the fission spectrum is illustrated in Fig. 9. A comparison of the data from the two experimental methods shows agreement within their statistical errors. Since this graph covers the lower energy

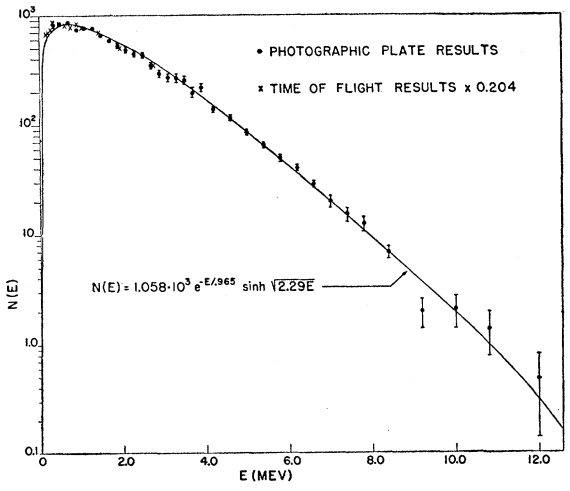

FIG. 7. Combined results showing fission neutron spectrum of U^{235} on a logarithmic scale over the energy range of 0.18 to 12 Mev.

[11] This figure was obtained by finding the normalization factor required to equalize the areas under each set of data over their common energy region of 0.35 to 2.7 Mev.

[12] The authors are indebted to B. Carlson and M. Goldstein for obtaining this formula.

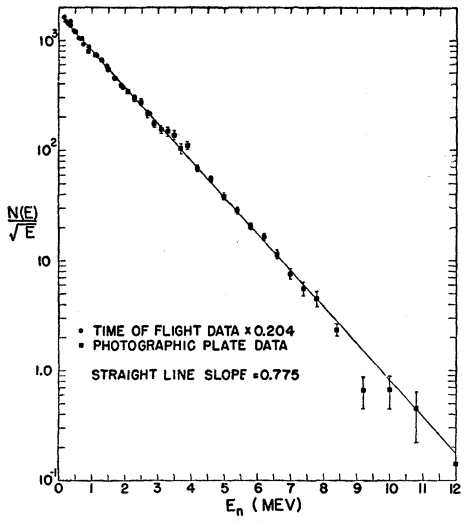

FIG. 8. Straight-line representation of fission neutron spectrum of U^{235} obtained by plotting $\ln N(E)/\sqrt{E}$ *vs* E.

range of the spectrum, the empirical relation of Fig. 8 have been used to illustrate the agreement with the data points.

If the results of the time-of-flight data are to be correctly interpreted and compared with the results of other methods, it is essential that the so-called "prompt" neutrons and gamma rays be prompt within a small fraction of the shortest flight time of interest. Also, it is required that the delayed neutrons and gamma rays be very few within the flight-time interval[13] or that they be delayed by times longer than the longest flight time of interest. It was reassuring, therefore, that a well defined gamma-ray peak was observed whose width was consistent with the time spread of the flight time measurements. It is reasonable to conclude that in the interval 0 to 1×10^{-8} sec there is no substantial number of delayed gamma rays.

In connection with the possible role of delayed gamma rays, it should also be noted that the sensitivity of the detector with its $\frac{1}{2}$ inch thick lead shield was considerably less for the fission gamma rays than for fission neutrons. Thus, according to Rose and Wilson,[14] there are about 6 fission gamma rays emitted within 0.1 μsec of fission compared to the value of 2.5 neutrons per fission. Assuming that most of the prompt fission gammas are in the resolved peak, and comparing the areas under the gamma-ray and neutron regions, one estimates the average sensitivity to gammas to be only 25% of that for neutrons. Thus, delayed gammas in the time range of interest, whose average energy was about

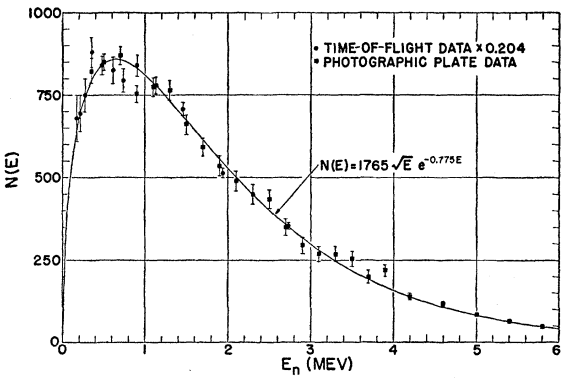

FIG. 9. Linear presentation of U^{235} fission neutron spectrum.

that for the prompt gammas, would not affect these data significantly unless they were in excess of about 10% of the prompt yield.

It should be noted that the time-of-flight data were taken for an energy of the primary neutrons of 5 to 80 kev, whereas the photographic plate data were taken with thermal neutrons. However, the evaporation model of fission, which has been applied with some success to calculations of fission spectra by Leachman,[15] suggests that this difference in bombarding energy should have negligible effect on the spectrum.

[13] Apparently, the literature contains no direct information on the delayed gamma rays from fission in the time range of 10^{-8} sec.

[14] See W. J. Whitehouse in *Progress in Nuclear Physics*, edited by O. R. Frisch (Pergamon Press, London, 1952).

[15] R. B. Leachman, Phys. Rev. **101**, 1005 (1956).